Reconfigurable Intelligent Surface Assisted MEC Offloading in NOMA-Enabled IoT Networks

Zhen Chen, *Senior Member, IEEE,* Jie Tang, *Senior Member, IEEE,* Miaowen Wen, *Senior Member, IEEE,* Zan Li, *Senior Member, IEEE,* Jun Yang, Xiu Yin Zhang, *Fellow, IEEE* and Kai-Kit Wong, *Fellow, IEEE*

***Abstract*—Integrating mobile edge computing (MEC) into the Internet of Things (IoT) enables resource-limited mobile terminals to offload part or all of the computation-intensive applications to nearby edge servers. On the other hand, by introducing reconfigurable intelligent surface (RIS), it can enhance the offloading capability of MEC, such that enabling low latency and high throughput. To enhance the task offloading, we investigate the MEC non-orthogonal multiple access (MEC-NOMA) network framework for mobile edge computation offloading with the assistance of a RIS. Different from conventional communication systems, we aim at allowing multiple IoT devices to share the same channel in tasks offloading process. Specifically, the joint consideration of channel assignments, beamwidth allocation, offloading rate and power control is formulated as a multi-objective optimization problem (MOP), which includes minimizing the offloading delay of computing-oriented IoT devices (CP-IDs) and maximizing the transmission rate of communication-oriented IoT devices (CM-IDs). Since the resulting problem is non-convex, we employ ϵ-constraint approach to transform the MOP into the single-objective optimization problems (SOP), and then the RIS-assisted channel assignment algorithm is developed to tackle the fractional objective function. Simulation results corroborate the benefits of our strategy, which can outperforms the other benchmark schemes.**

***Index Terms*—Reconfigurable intelligent surface (RIS), multi-objective optimization problem (MOP), mobile edge computing (MEC), non-orthogonal multiple access (NOMA).**

I. Introduction

THE prevalence of mobile devices and rapid growth of Internet of Things (IoT) have boosted an enormous application range, which are generated by edge devices in real-time, such as mobile phones, computers and sensors. However, since most of IoT devices always have limited computing capabilities, it is impractical to transmit and storage the local resource information. Mobile edge computing (MEC) as the most popular and realistic technology to relieve the prominent contradiction between service requirement and resource shortage, by providing real-time computing capabilities within the IoT network in close proximity to mobile subscribers [1]. Especially, computation offloading of MEC is a promising user-oriented use case to reduce the capital cost and provide flexibility.

In a MEC framework, the computation intensive or delay-sensitive tasks of each IoT device can be offload to the edge server instead of local execution, the performance of system (e.g., computation and latency requirements) was greatly enhanced [2]. Driven by the benefits of MEC, there were a large number of studies were emerged to solve joint communication and computation resource cooperation problems [3]–[5]. MEC is usually deployed at the network edge to provide fast-response data processing services and relieve the backhaul load. Therefore, MEC takes considerable advantages of offering energy savings for IoT devices, reducing the latency, achieving higher reliability [6]–[8]. In addition, MEC can be also beneficial to collect more information of interest about IoT location, preferences and behaviors, which can promote system to improve the quality of services (QoS) accordingly. The trend towards MEC is expected to accelerate as more computing-oriented devices and more intensive-oriented applications. Therefore, the emerging MEC paradigm is recognized as a key enabling technology, which has created an effective approach to realize IoT network.

Despite the benefits brought by MEC, the practical implementation of task offloading faces severe coverage and technical challenges. Due to the broadcast characteristics of wireless electromagnetic transmission, the computation tasks offloaded between IoT devices and the base station (BS) may be interrupt by nearby obstacles. This obviously could lead to severe the disruption risks to IoT devices [9]. The reconfigurable intelligent surface (RIS) is a promising technique to ensure the links of task offloading in MEC networks, due to its advantages of low cost, easy deployment and directional signal enhancement for the MEC service. By adjusting the phase shifts of RIS, incident signals can be dynamically reflected according to the requirements of

This work has been supported in part by National Key Research and Development Program of China under Grant 2019YFB1804100, in part by the National Natural Science Foundation of China under Grant 62001171, 61971194, 62222105, in part by the Engineering and Physical Sciences Research Council (EPSRC) under grant EP/V052942/1, in part by the Natural Science Foundation of Guangdong Province under Grant 2021A1515011966, 2022A1515011189, in part by the Special Project for Guangxi Science and Technology Bases and Talents under Grant AD21075054, in part by the Open Research Fund of Guangdong Key Laboratory of Aerospace Communication and Networking Technology under Grant 2018B030322004, in part by the Open Research Fund of State Key Laboratory of Integrated Services Networks, Xidian University (No. ISN23-05), and in part by the International Science and Technology Cooperation Project of Guangzhou (Huangpu) under Grant 2020GH06. (*Corresponding author: Jie Tang*.)

Z. Chen is with the School of Electronic and Information Engineering, South China University of Technology, Guangzhou, China, and also with the State Key Laboratory of Integrated Services Networks, Xidian University, Xian, China (e-mail:chenz@scut.edu.cn).

J. Tang, M. Wen and X. Zhang are with the School of Electronic and Information Engineering, South China University of Technology, Guangzhou, China (e-mail:eejtang@scut.edu.cn, pku.miaowenwen@gmail.com, zhangxiuyin@scut.edu.cn).

Z. Li is with the School of Electronics and Information Engineering, Xidian University, Xian, China (e-mail:zanli@xidian.edu.cn).

K.-K Wong is with the Department of Electronic and Electrical Engineering, University College London, London, United Kingdom. (e-mail: kaikit.wong@ucl.ac.uk).

systems [10]–[12]. Especially, authors in [13] proposed the cooperative reflection design for the RIS-aided multidevice MEC communications, which is the potential to significantly enhance the spectrum and energy efficiencies. Therefore, by exploiting the benefits of RIS, the potential of MEC can be significantly improved, including suppressing the channel interference, improving antenna gain and boosting the desired signal [14]–[16].

Another key characteristics of IoT is massive connection density. According to 3GPP standard for IoT projections, the number of the mobile devices will continue to rise and reach 20.8 billion, which will be an enormous challenge for the conventional orthogonal multiple access (OMA) to fulfill the massive dense connectivity requirement [17]. To resolve above challenge, non-orthogonal multiple access (NOMA) technique [5], [18], [19] was developed as an alternative for conventional OMA, due to the fact that it can be made much larger than the number of orthogonal resource elements therein and avoid severe delay. Thus, NOMA were actively investigated, which can accommodate multiple users over the limited number of available resources block, and exploit the successive interference cancelation (SIC) to reduce the co-channel interference.

Based on the above observations, MEC can provide a considerable platform to NOMA networks, and RIS well made up for the unstable wireless channels. As a result, it is necessary to investigate the task offloading and resource management for RIS-assisted MEC-NOMA system, while ensuring the offload transmission requirements of IoT devices. However, considering the requirements of disparities between power-limited IoT devices and the stringent computation, channel assignment and offloading decisions are required to be optimized properly. Besides, it is generally difficult to obtain channel state information (CSI) accurately in most applications [20], [21]. These observations motivate us to develop an RIS-assisted task offloading and channel assignment mechanism for MEC-NOMA network.

A. Related Works

Motivated by the aforementioned backgrounds, several pioneer MEC researches have been done to integrate MEC and NOMA into IoT communication network [5], [22]–[27]. Specifically, to reduce the total execution delay time, a joint SIC ordering and computation resource design was investigated in the NOMA-aware MEC networks [24]. The authors considered the single- and multiple-users scenarios for NOMA-enabled multi-access MEC network [28]. By properly offloading computation-task to the nearby MEC servers, the NOMA transmission-time and the offloading workloads were optimized, simultaneously. In [29], an asymptotically optimal online offloading algorithm was developed to maximize the long-term system utility in the NOMA-aided MEC network, while balancing user fairness and the throughput of system. The studies of [30] have combined MEC with network slicing to investigate the average revenue maximization problem. In [31], the authors put forward a resource scheduling-based algorithm for computation-offloading in the device-to-device (D2D)-aid MEC-NOMA communication, in which each IoT device can offload its computation task to relieve the high computing burden in D2D communications.

To further enhance the task offloading performance of the resource-limited users, a few works developed RISs to jointly optimize computing, phase shifts of RIS and communications, in which various types of modeling schemes were exploited, e.g., minimize latency [32], or maximize nonlinear learning error of the learning task [33]. For example, the authors in [32] and [34] proposed RIS-assisted MEC framework, in which the RIS is properly deployed to guarantee the QoS requirements of MEC services and system throughput. The authors in [35] proposed an RIS-assisted multi-user MEC architecture with multiplexing offloading to maximize the total completed task-input bits. Considering the limited computing capability of MEC-enabled network, [36] developed a cooperative communication-computation offloading strategy among IoT devices, which can reduce the total energy consumption considerably. Due to user mobility and dynamic demands, some part of hot-spot areas may cool down soon afterward over time.

However, for certain dense connection area, it is possible for multiple devices to request offloading services simultaneously. Under such circumstances, the channel resources are insufficient to assign one dedicated channel for each offloading IoT device. In addition, the short distances among the IoT devices result in strong mutual interference of frequency channels. Fortunately, the same channels can be time-shared by multiple IoT devices. To this end, we consider to decide the fraction of the transmitted data that each IoT devices should offload, and the fraction of channel time can assigned to each IoT device. Unfortunately, the existing works ignore channel assignments in computation services, which is greatly restrict task offloading in considered RIS-assisted MEC-NOMA scenario.

B. Motivation

In practical MEC-NOMA network, computing-oriented IoT devices (CP-IDs) and communication-oriented IoT devices (CM-IDs) usually are coexistence. The CP-IDs refer to the computing tasks of IoT devices that can be offloaded to nearby MEC servers. The CM-IDs usually refer to the communication tasks of IoT devices, who mainly focus on data rate. It should be noted that CM-IDs has strong timeliness. It is worth noting that if the transmitted time can be divided into a few of epochs, and the frequency channel is assigned to multiple IoT devices based on the epochs of time. It is benefit to enhance the procedure efficiency of CP-IDs and the real-time communication ability of CM-IDs. Motivated by the advantages of channel assignment, we focus on MEC offloading with channel assignment, where CP-IDs and CM-IDs will share the same channel resources to accomplish its offloading tasks.

In this paper, we investigate the channel assignment-based task offloading framework for the RIS-assisted MEC-NOMA system. The main contributions of this paper are summarized as follows.

- Different from the existing works about task offloading, we build an RIS-assisted MEC-NOMA offloading framework, where the channel assignment-based task offloading is proposed to more efficiently utilize the available system resources. In the proposed framework, a multi-objective optimization problem (MOP) is formulated to maximize the MEC task offloading, while ensuring the computation delay of successful task execution below a tolerable level.
- To obtain the feasible solution, the proposed MOP is decoupled into four independent subproblems by exploiting means of ϵ-constraint method. By deriving the explicit form of ϵ-constraint method, we employ the SIC and penalty function-based methods to solve the beamwidth allocation and offloading rate subproblems, iteratively, and the approximate closed-from solution is derived for the transmit power control subproblem.
- For the channel assignment problem, the time division criteria is designed in accordance with channel matching strategy, which is to guarantee that each channel is allocated for at most one IoT device. In the channel matching strategy, the channel assignment decision with offloading ratio scheme is developed to determine the optimum solution, while guarantee the fairness of completion time.

The remainder of this paper is organized as follows. Section II describes the system model, and the RIS-assisted MEC-NOMA offloading problem is formulated. In Section III, the problem formulation with channel assignment scheme is illustrated. The corresponding optimization algorithm is presented to solve the optimization problem in Section IV. Numerical results confirm the performance of the obtained solution in Section V. Finally, conclusions are given in Section VI.

II. System Model and Problem Formulation

As illustrated in Fig. 1, we consider the MEC in a RIS-assisted NOMA network. The BS equipped with an MEC server to provide computation services for the single antenna IoT devices, where MEC server is accessed through the assistance of a RIS. The IoT devices are randomly distributed in the cell, including CP-IDs and CM-IDs. The CP-IDs and CM-IDs are indexed in sets $\mathcal{I} = \{1, 2, ..., I\}$ and $\mathcal{J} = \{1, 2, ..., J\}$ respectively. I and J denote the number of CP-IDs and CM-IDs, respectively. In the following, we consider that the task at each IoT device $m \in \mathcal{M}$ can be arbitrarily partitioned into two portions for offloading and local computing, respectively, indexed by $\mathcal{M} = \{1, 2, ...M\}$. M is the number of IoT devices. There is only one application of each portion from each IoT device, such that the m'-th application is always from the m-th IoT device. The computation of IoT device m may offload to the MEC server with the corresponding channels.

A. RIS-assisted channel

Due to the multi-path effect and intrinsic random feature of channel, the transmitted data may suffer from high propagation loss, when the occlusion occurred between the IoT devices and the MEC server [37]. To this end, we consider the RIS to configure the channel by dynamically adjusting the phase shift of each reflecting element; thus, the signal from IoT device k to the BS includes both the direct link (Device-BS link) and the reflected links (Device-RIS-BS links), where the reflected link consists of the device side, the phase shifts of RIS, and the RIS-BS side [38]. According to the characteristics of RIS, we assume that the beamforming is reflected at the RIS without beamforming gain loss. For each pair, the transmit and receive beams are required to be aligned toward each other, which is measured relative to perfect beam alignment. Both transmitter and receiver antenna arrays have the same half power beamwidth (HPBW), which corresponds to the angular aperture of the main beam. Inspired by [39], we simplify the actual antenna pattern by the sectorized gain pattern based on the realistic pattern of ULA for the sake of mathematical tractability. Thus, for a ULA with ℓ antenna elements, the half power beamwidth can be expressed as a function of ℓ as follows [40]

Fig. 1. RIS-assisted MEC offloading in NOMA-enabled IoT networks.

$$\theta(\ell) = 2\left(\frac{\pi}{2} - \arccos\frac{2.784}{\ell\pi}\right) \approx \frac{1.7723}{\ell}. \tag{1}$$

Thus it is widely used for coverage and rate analysis of RIS-assisted wireless networks, which the antenna gain of signal transmission can be given by

$$G = \underbrace{g_{\mathrm{id}} g_{\mathrm{RIS}_t}}_{\mathrm{id-RIS\ link}} \underbrace{g_{\mathrm{RIS}_r} g_{\mathrm{bs}}}_{\mathrm{RIS-BS}}, \tag{2}$$

where g_{id} and g_{bs} denote the main lobe gain of IoT device and BS, respectively. g_{n}, $\mathrm{n} \in \{\mathrm{RIS}_t, \mathrm{RIS}_r\}$, denotes the main lobe gain of RIS. Furthermore, we have

$$\begin{aligned} g_{\mathrm{id}} &= \frac{2\pi - (2\pi - \theta(\ell_{\mathrm{id}}))\, z_{\mathrm{id}}}{\theta(\ell_{\mathrm{id}})}, \\ g_{\mathrm{bs}} &= \frac{2\pi - (2\pi - \theta(\ell_{\mathrm{bs}}))\, z_{\mathrm{bs}}}{\theta(\ell_{\mathrm{bs}})} \\ g_{\mathrm{n}} &= \frac{2\pi - (2\pi - \theta(\ell_{\mathrm{n}}))\, z_{\mathrm{RIS}}}{\theta(\ell_{\mathrm{n}})}. \end{aligned} \tag{3}$$

where z_{id}, z_{bs} and z_{RIS} denote side lobe gains of IoT device, BS and RIS, respectively. $\theta(\ell_{\mathrm{id}})$, $\theta(\ell_{\mathrm{bs}})$ and $\theta(\ell_{\mathrm{n}})$ are the HPBW of user, BS and RIS, respectively. Since RIS can

be deployed in advance, the small-scale fading channel is considered to between RIS and BS link. In addition, $\theta(\ell_{\mathrm{id}})$ can be ignored with the single antenna IoT devices. Thus, we consider the HPBW of RIS $\theta(\ell_{\mathrm{RIS}_t})$ as a variable to be optimized, while fixed the HPBW of BS $\theta(\ell_{\mathrm{bs}})$ and $\theta(\ell_{\mathrm{RIS}_r})$ in the following.

Let a set of channels be $\mathcal{K} = \{1, 2, \ldots, K\}$, the k th channel is indexed by $k \in \mathcal{K}$ and K denotes the total number of channels. For simplicity, we define channel indicator as $x_{m,k} \in \{0, 1\}$. If $x_{m,k} = 1$, it means that IoT device m is assigned to channel k and $x_{m,k} = 0$, otherwise. Each offloaded IoT device is assigned to at most one channel. We have

$$\sum_{k \in \mathcal{K}} x_{m,\,k} \leq 1, \quad m \in \{i, j\}. \tag{4}$$

In order to support more IoT devices offloading, the channel assignment is exploited to multiple IoT devices that can offload tasks with the same channel. Restricted by limited geographical area, it is inevitable for strong interference of channel during simultaneous transmissions. Instead, the channel can be divided into a few of epochs, and each IoT device can select a time epochs of channel for each application. Let $\mathrm{y}_{m,k}$ be the fraction of the channel time, the IoT device m is assigned to channel k, which can be given by

$$\sum_{m \in \mathcal{M}} \mathrm{y}_{m,k} \leq 1. \tag{5}$$

We assume that variable $\mathrm{y}_{m,k}$ satisfies $\mathrm{y}_{m,k} \in [0, 1]$. It is obvious that if the time granularity of the channel is sufficiently small, thus the relationship between x_{mk} and $\mathrm{y}_{m,k}$ can be derived

$$\begin{cases} \text{if } \mathrm{y}_{m,\,k} \in (0, 1], & \text{then } x_{m,\,k} = 1, \\ \text{if } x_{m,\,k} = 0, & \text{then } \mathrm{y}_{m,\,k} = 0. \end{cases} \tag{6}$$

It follows that if $\mathrm{y}_{m,\,k}$ satisfies $\mathrm{y}_{m,\,k} \in (0, 1]$, the corresponding channel k is assigned to IoT device m; On the contrary, if the channel size is set as $x_{m,\,k} = 0$, channel k will not be assigned to IoT device m. Based on these observation, we have the following equivalent relationship

$$\epsilon_1 < \mathrm{y}_{m,\,k} \leq x_{m,\,k} + (1 - x_{m,\,k})\,\epsilon_1 \tag{7}$$

with $\epsilon_1 = 0$. When $\mathrm{y}_{m,\,k} \in (0, 1]$, it is observed that the left of (7) holds, and then $x_{m,\,k} = 1$ must be holds to satisfy the right of (7); On the contrary, when $x_{m,\,k} = 0$, both the left and right sides of (7) are zero. Therefore, $\mathrm{y}_{m,\,k} = 0$ must be holds.

Based on the above analysis, to avoid the channel interference of CM-ID link, we need to decode the transmitted signal of CP-ID by using the principle of SIC, which is a widely used assumption in the existing literatures [41]–[45]. Specifically, CP-ID sequentially decodes the signal from devices with higher channel gains and regards all the other signals (including CM-ID signal) as the interference, and then removes their messages one by one. Furthermore, let us assume that the decoding order of the SIC at a receiver does not change as long as each user's minimum SINR requirement (i.e. minimum decoding threshold) is met, which is a commonly-used assumption in the existing works such as [40]. Thus, the corresponding SINR for active IoT devices can be given by

$$\gamma_{i,k} = \frac{x_{i,k} p_{i,k} G_{i,k} \left|h_{i,k}\right|^2 L_i}{\underbrace{\sum_{\substack{i' \in \mathcal{I}, \\ i' \neq i}} x_{i',k} p_{i',k} G_{i',k} \left|h_{i',k}\right|^2 L_{i'}}_{\text{CP}-\text{ID interference}} + \underbrace{\sum_{j \in \mathcal{J}} x_{j,k} p_{j,k} G_{j,k} \left|h_{j,k}\right|^2 L_j}_{\text{CM}-\text{ID interference}} + \sigma_0}, \tag{8}$$

$$\gamma_{j,k} = \frac{x_{j,k} p_{j,k} G_{j,k} \left|h_{j,k}\right|^2 L_j}{\sum_{j' \in \mathcal{J}, j' \neq j} x_{j',k} p_{j',k} G_{j',k} \left|h_{j',k}\right|^2 L_{j'} + \sigma_0}, \tag{9}$$

where $p_{i,k}$ and $p_{j,k}$ denote the transmit power for CP-ID i and CM-ID j. L_i and L_j are the large-scale fading gain of IoT device i and j, respectively. Note that, $h_{i,k}$ and $h_{j,k}$ are small-scale fading gains for IoT device i and j. The noise is characterized by a additive white Gaussian noise (AWGN) variable with σ_0 being the noise power. $G_{i,k}$ and $G_{j,k}$ denote the antenna gain of the CP-ID i and CM-ID j, respectively.

According to the (8) and (9), the data transmission rate $R_{i,\,k}$ and $R_{j,\,k}$ can be given below

$$R_{ii,\,k} = W \log_2 \left(1 + \gamma_{ii,\,k}\right), \quad ii \in \{i, j\} \tag{10}$$

where W denotes the bandwidth of system.

It follows that the average transmission rate for CP-ID i at channel k is $\mathrm{y}_{i,k} R_{i,\,k}$. when the channel time $\mathrm{y}_{i,k}$ is used.

B. Task Computing Model

Define $0 \leq \lambda_{i,\,k} \leq 1$ as the offloading rate of CP-ID i assigned to channel k. By introducing a variable $0 < \epsilon_2 \ll 1$ and defining the following relationship

$$\epsilon_2 x_{i,\,k} \leq \lambda_{i,\,k} \leq x_{i,\,k}, \tag{11}$$

where $x_{i,\,k}$ is the indicator, whose role is to assign appropriate channel for active IoT device. Specifically, the indicator $x_{i,\,k} = 1$ means that the CP-ID i is assigned to channel k; otherwise, $x_{i,\,k} = 0$. Thus, we can obtain

$$\begin{cases} \lambda_{i,\,k} \in (0, 1] \Longleftrightarrow x_{i,\,k} = 1 \\ \lambda_{i,\,k} = 0 \quad\;\; \Longleftrightarrow x_{i,\,k} = 0 \end{cases} \tag{12}$$

Let D_i be the amount of data to be processed for application i. Given the offloading rate relationship between the computation load and communication data, the offloaded task is transmitted in consistent with channel k, denoted by $\lambda_{i,\,k} D_i$, and the transmission time of channel k for this uploading data can be written as

$$\tau^U_{i,\,k} = x_{i,\,k} \frac{\lambda_{i,\,k} D_i}{\mathrm{y}_{i,\,k} R_{i,\,k}}. \tag{13}$$

To prevent having zero denominator in (13), we rewrite the variable ϵ_1 that to be satisfied in range of $0 < \epsilon_1 \ll 1$. Thus, the transmitted energy of IoT device i is given by

$$E^U_i = \sum_{k \in \mathcal{K}} P_i \tau^U_{i,k} = \sum_{k \in \mathcal{K}} \frac{x_{i,k} \lambda_{i,k}}{\mathrm{y}_{i,k}} \frac{P_i D_i}{R_{i,k}}, \tag{14}$$

where P_i denotes the maximum transmit power of user i.

The local energy consumption is determined by the execution time of CPU and power overhead. Inspired by [46], the power overhead is expressed as $\kappa \left(f_i^L\right)^3$, where f_i^L denotes the computational CPU speed of IoT device i and κ denote the energy conversion coefficient. Based on this sake, the local execution time for application i can be described as

$$\tau_i^L = \frac{\left(1 - \sum_{k\in\mathcal{K}} x_{i,k}\lambda_{i,\,k}\right)\kappa D_i}{f_i^L}. \tag{15}$$

The local energy consumption of IoT device i for computation can be written as

$$E_i^L = \kappa D_i \left(f_i^L\right)^2 \left(1 - \sum_{k\in\mathcal{K}} x_{i,k}\lambda_{i,k}\right). \tag{16}$$

Combined (14) and (16), the total energy consumption of IoT device m is

$$\begin{aligned} E_i &= E_i^L + E_i^U \\ &= \mathcal{E}_i^L \left(1 - \sum_{k\in\mathcal{K}} x_{i,\,k}\lambda_{i,k}\right) + \sum_{k\in\mathcal{K}} \frac{x_{i,\,k}\lambda_{i,\,k}}{\mathrm{y}_{i,\,k}} \mathcal{E}_{i,\,k}^U \end{aligned} \tag{17}$$

where $\mathcal{E}_i^L = \kappa D_i \left(f_i^L\right)^2$ and $\mathcal{E}_{i,\,k}^U = \frac{P_i D_i}{R_{i,\,k}}$.

For the execution time of MEC server, the data transmission assign to channel k is mathematically cast as:

$$\tau_{i,k}^P = \frac{x_{i,k}\lambda_{i,k}\kappa D_i}{f_s}, \tag{18}$$

where f_s is the processing capacity of the MEC server.

C. Problem Formulation

In this subsection, we formulate the channel assignment-based task offloading for RIS-assisted MEC-NOMA network. As discussed before, we assume that the total delay of each CP-ID consists of the beam alignment time τ_0, the offloading task time $\tau_{i,k}^U$, and the computation time of MEC server $\tau_{i,k}^P$. Thus, the total delay time of CP-IDs i within the assigned channel k can be calculated as

$$\tau_i = \tau_0 + \tau_{i,k}^U + \tau_{i,k}^P, \tag{19}$$

where τ_0 is the execution time on the beam alignment of IoT devices. By exploiting the point-to-point strategy, the beam alignment time τ_0 is

$$\begin{aligned} \tau_0 &= \sum_{\forall i\in\mathcal{I}} \left\lceil \frac{\Psi_{\mathrm{id}}}{\theta(\ell_{t,i})} \right\rceil T_p + \sum_{\forall j\in\mathcal{J}} \left\lceil \frac{\Psi_{\mathrm{id}}}{\theta(\ell_{t,j})} \right\rceil T_p \\ &\approx T_p \Psi_{\mathrm{id}} \left(\sum_{\forall i\in\mathcal{I}} \frac{1}{\theta(\ell_{t,i})} + \sum_{\forall j\in\mathcal{J}} \frac{1}{\theta(\ell_{t,j})} \right), \end{aligned} \tag{20}$$

where Ψ_{id} is sector-level beamwidth at UE side, $\theta(\ell_{t,i})$ and $\theta(\ell_{t,j})$ are beamwidth of RIS towards the CP-ID i and CM-ID j, respectively. $\tau_{i,k}^U$ in (19) is the offloading task time of CP-ID i to be assigned to channel k, which can be given by (13). T_p is the time required for a pilot transmission.

Based on the above analysis, the following problem formulation should be satisfied: 1) maximizing the total spectral efficiency of CM-IDs; 2) minimizing the average delay of CP-IDs. Defining $\mathcal{P} = \{p_{i,\,k}$ and $p_{j,\,k}, \forall i \in \mathcal{I}, \forall j \in \mathcal{J}, \forall k \in \mathcal{K}\}$ includes power allocation variables, $\Lambda = \{\lambda_{i,k}, \forall i \in \mathcal{I}, \forall k \in \mathcal{K}\}$ includes offloading rate variables and $\Omega = \{\theta(\ell_{t,i,k})$ and $\theta(\ell_{t,j,k}), \forall i \in \mathcal{I}, \forall j \in \mathcal{J}, \forall k \in \mathcal{K}\}$ includes beamwidth allocation variables, the MOP can be mathematically cast as

$$\mathbb{P}_0 : \min_{\mathcal{X},\mathcal{P},\Lambda,\Omega} \left\{ \frac{\sum_{i\in\mathcal{I}} \beta_i \tau_i}{I} \right\} \tag{21a}$$

$$\max_{\mathcal{X},\mathcal{P},\Lambda,\Omega} \left\{ \sum_{j\in\mathcal{J}} \sum_{k\in\mathcal{K}} x_{j,k} R_{j,k} \right\} \tag{21b}$$

s.t.

$$x_{i,k} \in \{0,1\}, x_{j,k} \in \{0,1\}, \forall i \in \mathcal{I}, \forall j \in \mathcal{J}, \forall k \in \mathcal{K} \tag{21c}$$

$$\sum_{k\in\mathcal{K}} x_{i,k} = \sum_{k\in\mathcal{K}} x_{j,k} = 1, \quad \forall i \in \mathcal{I}, \forall j \in \mathcal{J} \tag{21d}$$

$$\sum_{i\in\mathcal{I}} x_{i,k} + \sum_{j\in\mathcal{J}} x_{j,k} \le M_k, \quad \forall i \in \mathcal{I}, \forall j \in \mathcal{J} \tag{21e}$$

$$0 < \lambda_{i,k} \le 1, \quad \forall i \in \mathcal{I} \tag{21f}$$

$$\tau_i \le T_i, \quad \forall i \in \mathcal{I} \tag{21g}$$

$$\tau_i^L \le T_i, \quad \forall i \in \mathcal{I} \tag{21h}$$

$$\sum_{k\in\mathcal{K}} x_{j,k} R_{j,k} \ge R_0, \quad \forall j \in \mathcal{J} \tag{21i}$$

$$E_i^L + \tau_{i,k}^U p_{i,k} \le E_i, \quad \forall i \in \mathcal{I} \tag{21j}$$

$$\theta_0 \le \theta(\ell_{t,i,k}) \le \theta_1, \quad \forall i \in \mathcal{I} \tag{21k}$$

$$\theta_0 \le \theta(\ell_{t,j,k}) \le \theta_1, \quad \forall j \in \mathcal{J} \tag{21l}$$

$$0 \le p_{i,k} \le P_i, \quad \forall i \in \mathcal{I} \tag{21m}$$

$$0 \le p_{j,k} \le P_j, \quad \forall j \in \mathcal{J} \tag{21n}$$

where β_i is the energy consumption weight coefficients of CP-IDs, which satisfies $\sum_{i\in\mathcal{I}} \beta_i = 1$. The objective function (21a) denotes the average offloading delay of CP-IDs $\tau_{\mathrm{avg}} = \frac{\sum_{i\in\mathcal{I}} \beta_i \tau_i}{I}$, (21b) denotes the total data transmission rate of CM-IDs. For ease of notation, $\mathcal{X} = \{x_{i,k}, \forall i \in \mathcal{I}, \forall k \in \mathcal{K}\}$ includes the CP-IDs assignment variables. The constraint (21c) guarantee that each channel is allocated for at most one CP-ID, while the constraint (21d) ensure that each CP-ID is selected by one channel. The constraint (21e) means the maximum number of IoT devices on a channel k. Constraint (21e) shows the size of channel k, i.e., $M_k = 1$. Constraints (21g) (21h) ensure that the offloading can be completed in time requirement of T_i. The constraint (21i) ensures that the instantaneous transmission rate of CM-IDs is larger than R_0. R_0 denotes the minimum requirements of the offloaded bits of each IoT device. In constraint (21j), we introduce total energy consumption E_i to constraint the CP-IDs and CM-IDs. Constraint (21k) and (21l) ensure the maximum and minimum beamwidth requirements for the RIS. θ_0 and θ_1 are the maximum beamwidth of RIS. The maximum power constraint of the CP-IDs and CM-IDs is given in (21m) and (21n), respectively.

Note that the objective functions (21a) and (21a) is in conflict with each other. To solve this issue, the MOP can be adopted to find a solution that satisfies the predefined

conditions of Pareto optimality. Then, the ϵ-constrain method is employed to transform the proposed MOP into a single-objective optimization problem (SOP). By introducing the constraint to the objective function (21b), the problem $\mathbb{P}_0$ can be recast as follows

$$\mathbb{P}_1 : \min_{\mathcal{X},\mathcal{P},\Lambda,\Omega} \{\tau_{\text{avg}}\}, \tag{22a}$$

$$s.t., (21c) - (21n)$$

$$-R_{\text{tot}} \leq \epsilon = -R_1, \tag{22b}$$

where the constraint (22b) is to ensure that total transmission rate of CM-IDs should be greater than R_1, and R_{tot} is the total data transmission rate of CM-IDs.

Lemma A. *If τ_{avg} exists for all $(\mathcal{X}, \mathcal{P}, \Lambda, \Omega)$, $(\mathcal{X}^*, \mathcal{P}^*, \Lambda^*, \Omega^*)$ is Pareto optimal solution of the MOP if and only if there exists ϵ such that $(\mathcal{X}^*, \mathcal{P}^*, \Theta^*, \Omega^*)$ is the unique optimal solution to the SOP.*

Proof: The proof is given in Appendix A. ∎

The Lemma A establishes the Pareto optimal solutions of the proposed MOP (22) with ϵ-constrain strategy, which is given by Appendix A. It concludes that the ϵ-constraint method in Lemma A guarantee the Pareto optimal solutions of the MOP.

By considering the time fairness, we split the minimum transmission rate R_1 in (22b) with regard to the transmission requirements of each CM-ID. Substituting (21i) into (22b), the corresponding optimization problem in $\mathbb{P}_1$ is reformulated, which yields the following optimization problem

$$\mathbb{P}_2 : \min_{\mathcal{X},\mathcal{P},\Lambda,\Omega} \{\tau_{\text{avg}}\} \tag{23a}$$

$$s.t.,$$

$$x_{i,k} \in \{0,1\}, x_{j,k} \in \{0,1\}, \forall i \in \mathcal{I}, \forall j \in \mathcal{J}, \forall k \in \mathcal{K} \tag{23b}$$

$$\sum_{k\in\mathcal{K}} x_{i,k} = \sum_{k\in\mathcal{K}} x_{j,k} = 1, \quad \forall i \in \mathcal{I}, \forall j \in \mathcal{J} \tag{23c}$$

$$\sum_{i\in\mathcal{I}} x_{i,k} + \sum_{j\in\mathcal{J}} x_{j,k} \leq M_k, \quad \forall i \in \mathcal{I}, \forall j \in \mathcal{J} \tag{23d}$$

$$0 < \lambda_{i,k} \leq 1, \quad \forall i \in \mathcal{I} \tag{23e}$$

$$\tau_i \leq T_i, \quad \forall i \in \mathcal{I} \tag{23f}$$

$$\tau_i^L \leq T_i, \quad \forall i \in \mathcal{I} \tag{23g}$$

$$\sum_{k\in\mathcal{K}} x_{j,k} R_{j,k} \geq \max\{R_0, \gamma_j R_1\}, \quad \forall j \in \mathcal{J} \tag{23h}$$

$$E_i^L + \tau_i^P p_{i,k} \leq E_i, \quad \forall i \in \mathcal{I} \tag{23i}$$

$$\omega_1 \leq \omega_{i,k} \leq \omega_0, \quad \forall i \in \mathcal{I} \tag{23j}$$

$$\omega_1 \leq \omega_{j,k} \leq \omega_0, \quad \forall j \in \mathcal{J} \tag{23k}$$

$$0 \leq p_{i,k} \leq P_i, \quad \forall i \in \mathcal{I} \tag{23l}$$

$$0 \leq p_{j,k} \leq P_j, \quad \forall j \in \mathcal{J} \tag{23m}$$

where γ_j in constraint (23h) denotes the transmission rate proportion of CM-ID j and satisfies $\sum_{j\in\mathcal{J}} \gamma_j = 1$. Note that the constraint $\omega_0 = 1/\theta_0$, $\omega_{i,\,k} = 1/\theta_{i,\,k}(\ell_t)$ and $\omega_{j,\,k} = 1/\theta_{j,\,k}(\ell_r)$, $\omega_1 = 1/\theta_1$ in (23j) and (23k) are a transformation of (21k) and (21l), respectively.

III. Joint power control and channel allocation design

In this section, our goal is to find the locally optimal solution of the problem $\mathbb{P}_2$. It is observed that when the MOP in (21) is transformed into the problem $\mathbb{P}_2$, the problem is still non-convex because of the channel assignment variable $\mathcal{X}$, offloading rate Λ, powers allocation $\mathcal{P}$ and beamwidth allocation Ω constraints. To solve the non-convex multi-variable problem $\mathbb{P}_2$, the SCA-based alternating optimization scheme is employed to divide problem $\mathbb{P}_2$ into four subproblems, which can be implemented as follows.

A. Beamwidth Allocation

We focus on the beamwidth allocation problem in this subsection. With the given channel assignment $\mathcal{X}$, power allocation P and offloading rate Λ, then, by introducing an auxiliary variable z, the problem $\mathbb{P}_2$ with regard to beamwidth allocation can be simplified into

$$\mathbb{P}_3 : \{\Omega^*\} = \underset{\Omega,z}{\text{argmin}} \{z \mid \mathcal{X}^*, \mathcal{P}^*, \Lambda^*\}, \tag{24a}$$

$$s.t. \quad \tau_i \leq T_i, \forall i \in \mathcal{I}, \tag{24b}$$

$$\sum_{k\in\mathcal{K}} x_{j,\,k} R_{j,\,k} \geq \max\{R_0, \gamma_j R_1\}, \forall j \in \mathcal{J}, \tag{24c}$$

$$E_i^L + \tau_i^U p_{i,k} \leq E_i, \forall i \in \mathcal{I}, \tag{24d}$$

$$\omega_1 \leq \omega_{i,k} \leq \omega_0, \forall i \in \mathcal{I}, \tag{24e}$$

$$\omega_1 \leq \omega_{j,k} \leq \omega_0, \forall j \in \mathcal{J}, \tag{24f}$$

$$\tau_{\text{avg}} \leq z. \tag{24g}$$

Obviously, the problem (24) is still non-convex combinatorial minimization problem due to the constraints (24b), (24d) and (24g). To solve this issue, we introduce an auxiliary variable u_i, which satisfies (25). According to (18) and (19), for $\forall i \in \mathcal{I}$, the constraints (24b), (24d) and (24g) can be re-written as

$$\tau_0 + \sum_{k\in\mathcal{K}} \frac{x_{i,k}\lambda_{i,k} D_i}{\mathrm{y}_{i,k} R_{i,k}} + \frac{x_{i,k}\lambda_{i,k}\kappa D_i}{f_s} \leq T_i, \tag{26}$$

$$E_i^L + \sum_{k\in\mathcal{K}} \frac{x_{i,k}\lambda_{i,k} D_i p_{i,k}}{W \mathrm{y}_{i,k} \log_2(1+u_i)} \leq E_i, \tag{27}$$

$$\tau_0 + \frac{1}{WI} \sum_{\forall i\in\mathcal{I}} \frac{\sum_{k\in\mathcal{K}} x_{i,k}\lambda_{i,k} D_i}{\log_2(1+u_i)} + \frac{1}{I} \sum_{\forall i\in\mathcal{I}} \frac{x_{i,k}\lambda_{i,k}\kappa D_i}{f_s} \leq z. \tag{28}$$

It can be verified that (26), (27) and (28) are convex. For the constraint (25), we introduce another auxiliary variable v, then the constraint (25) can be further transformed as follows

$$u_i v \leq x_{i,k} p_{i,k} G_{i,k} |h_{i,k}|^2 L_i, \tag{29}$$

where

$$v \geq \sum_{i'\in\mathcal{I}, i'\neq i} x_{i',k} p_{i',k} G_{i',k} |h_{i',k}|^2 L_{i'} + \sum_{j\in J} x_{j,k} p_{j,k} G_{j,k} |h_{j,k}|^2 L_j + \sigma_0. \tag{30}$$

$$u_i \leq \frac{x_{i,\,k} p_{i,k} G_{i,k} \left|h_{i,k}\right|^2 L_i}{\sum_{i' \in \mathcal{I}, i' \neq i'} x_{i',k} p_{i',k} G_{i',k} \left|h_{i',k}\right|^2 L_{i'} + \sum_{j \in \mathcal{J}} x_{j,\,k} p_{j,k} G_{j,k} \left|h_{j,k}\right|^2 L_j + N_0} \tag{25}$$

The upper bound of $u_i v$ is recast as follows

$$u_i v \leq \frac{v^{(t)}}{2u_i^{(t)}} x_i^2 + \frac{u_i^{(t)}}{2v^{(t)}} v^2, \tag{31}$$

where $u_i^{(t)}$ and $v^{(t)}$ are t-th iteration results of the u_i and v, respectively. Further, the (29) can be given by following convex constraint

$$\frac{v^{(t)}}{2u_i^{(t)}} u_i^2 + \frac{u_i^{(t)}}{2v^{(t)}} v^2 \leq x_{i,k} p_{i,k} G_{i,k} \left|h_{i,k}\right|^2 L_i \tag{32}$$

Further, we can reformulate problem $\mathbb{P}_3$ as:

$$\mathbb{P}_4 : \{\Omega^*\} = \underset{\Omega, z, u_i, v}{\operatorname{argmin}} \{z \mid \mathcal{X}^*, P^*, \Lambda^*\} \tag{33}$$

$$s.t. \quad (24c), (24e), (24f), (26), (27), (28), (29), (31).$$

It is observed that the resulting problem $\mathbb{P}_4$ is a convex optimization problem, and then the standard convex optimization method is applied to solve it. On the other hand, due to the existence of constraint (32), the solution of the problem $\mathbb{P}_3$ can be achieved by solving the the problem $\mathbb{P}_4$ iteratively. The convergence of the beamwidth allocation algorithm can be proved in [47].

B. Offloading rate updating

In this subsection, we focus on the offloading rate optimization problem while regarding $\mathcal{X}$, $\mathcal{P}$ and Ω as fixed values. The problem $\mathbb{P}_2$ will be transformed to the offloading rate allocation subproblem

$$\mathbb{P}_5 : \{\Lambda^*\} = \underset{\Lambda}{\operatorname{argmin}} \{\tau_{\text{avg}} \mid \mathcal{X}^*, \mathcal{P}^*, \Omega^*\} \tag{34a}$$

$$0 < \lambda_i \leq 1, \forall i \in \mathcal{I}, \tag{34b}$$

$$\tau_i \leq T_i, \forall i \in \mathcal{I}, \tag{34c}$$

$$\tau_i^L \leq T_i, \forall i \in \mathcal{I}, \tag{34d}$$

$$E_i^L + \tau_i^U p_{i,k} \leq E_i, \forall i \in \mathcal{I}, \tag{34e}$$

where

$$\tau_{\text{avg}} = \tau_0 + \frac{1}{I} \sum_{\forall i \in \mathcal{I}} \frac{\sum_{k \in \mathcal{K}} x_{i,k} \lambda_{i,k} D_i}{R_{i,k}} + \frac{1}{I} \sum_{\forall i \in \mathcal{I}} \frac{x_{i,k} \lambda_{i,k} \kappa D_i}{f_s}.$$

Note that the objective function τ_{avg} of the problem $\mathbb{P}_5$ is a monotonically increasing function of $\lambda_{i,k}$. Therefore, the lower bound of $\lambda_{i,k}$ can be easily obtained from (34c), which can be expressed as:

$$\lambda_{i,k} \leq \frac{\sum_{k \in \mathcal{K}} x_{i,k} R_{i,k} f_s \left(T_i - \tau_0\right)}{f_s D_i + \kappa \sum_{k \in \mathcal{K}} x_{i,k} R_{i,k} D_i}. \tag{35}$$

Substituting (34e) into (35), we have

$$\lambda_{i,k} \leq \frac{\left(E_i - \kappa {f_i}^2 D_i\right) \sum_{k \in \mathcal{K}} x_{i,k} R_{i,k}}{D_i p_{i,k} + \kappa {f_i}^2 D_i \sum_{k \in \mathcal{K}} x_{i,k} R_{i,k}}. \tag{36}$$

Combined (34b), (35) with (36), it clearly has a upper bound of λ_i as (37).

Furthermore, using (15) and (34d), we have

$$\lambda_i \geq 1 - \frac{T_i f_i}{\kappa D_i}. \tag{38}$$

Therefore, the optimal solution is obtained by taking the a lower bound value of λ_i. That is

$$\lambda_i \geq \max\left\{1 - \frac{T_i f_i}{\kappa D_i}, 0\right\}. \tag{39}$$

C. Powers allocation updating

In this subsection, we aim to obtain the approximate optimal solution of the power allocation problem. With the given channel assignment $\mathcal{X}$, offloading rate Λ and channel assignment Ω, the problem $\mathbb{P}_2$ is mathematically recast as

$$\mathbb{P}_6 : \{\mathcal{P}^*\} = \underset{\mathcal{P}}{\operatorname{argmin}} \{\tau_{\text{avg}} \mid \mathcal{X}^*, \Lambda^*, \Omega^*\} \tag{40a}$$

$$s.t. \quad \tau_i \leq T_i, \forall i \in \mathcal{I} \tag{40b}$$

$$\sum_{k \in \mathcal{K}} x_{j,\,k} R_{j,\,k} \geq \max\left\{R_0, \gamma_j R_1\right\}, \forall j \in \mathcal{J} \tag{40c}$$

$$E_i^L + \tau_i^U p_{i,k} \leq E_i, \forall i \in \mathcal{I} \tag{40d}$$

$$0 \leq p_{i,k} \leq P_i, \forall i \in \mathcal{I} \tag{40e}$$

$$0 \leq p_{j,k} \leq P_j, \forall j \in \mathcal{J} \tag{40f}$$

Accordingly, based on the (20) and (10), it can be seen that the objective function τ_{avg} of $\mathbb{P}_5$ is a monotonically reducing function of $p_{i,k}$, and is a monotonically increasing function of $p_{j,k}$. Therefore, the solution of $\mathbb{P}_6$ is obtained by taking the lower bound of $p_{j,k}$. From the constraint (40b), the power $p_{j,k}$ should be satisfies (41). With the above constraint (40c), we derive

$$p_{j,k} \geq \left(2^{\frac{R_j^{\max}}{W}} - 1\right) \frac{\sum\limits_{j' \in \mathcal{I}, j' \neq j} x_{j',k} p_{j',k} G_{j',k} \left|h_{j',k}\right|^2 L_{j'} + \sigma_0}{G_{j,k} \left|h_{j,k}\right|^2 L_j} \tag{42}$$

where $R_j^{\max} = \max\left\{R_0, \gamma_j R_1\right\}$. Based on the above analysis, the lower bound of $p_{j,k}$ can be written as follows

$$p_{j,k}^{\min} = \left(2^{\frac{R_j^{\max}}{W}} - 1\right) \frac{\sum\limits_{j' \in \mathcal{I}, j' \neq j} x_{j',k} p_{j',k}^{\min} G_{j',k} \left|h_{j',k}\right|^2 L_{j'} + \sigma_0}{G_{j,k} \left|h_{j,k}\right|^2 L_j} \tag{43}$$

Combined (16), (40d) and (43), we have (44). Form the (44), the upper bound of $p_{i,k}$ is obtained stems from an increasing function with regard to the power $p_{i,k}$. Based on this observation, the Lambert-$\mathcal{W}$ function is exploited to obtain the optimal $p_{i,k}$. After some algebra manipulations, we obtain the following solution

$$p_{i,k}^{\max} = -\frac{\Xi_A \times \mathcal{W}\left(\Xi_F \times 2^{\Xi_E}\right)}{\Xi_C} - \Xi_G, \tag{45}$$

$$\lambda_i \leq \min\left\{\frac{\sum_{k\in\mathcal{K}} x_{i,k}R_{i,k}f_s\left(T_i-\tau_0\right)}{f_sD_i+\kappa\sum_{k\in\mathcal{K}} x_{i,k}R_{i,k}D_i}, \frac{\left(E_i-\kappa {f_i}^2 D_i\right)\sum_{k\in\mathcal{K}} x_{i,k}R_{i,k}}{D_ip_{i,k}+\kappa {f_i}^2 D_i\sum_{k\in\mathcal{K}} x_{i,k}R_{i,k}}, 1\right\} \tag{37}$$

$$p_{i,k} \geq \left[2^{\frac{\lambda_{i,k}D_if_s}{\left(f_sT_i-f_s\tau_0-\lambda_{i,k}\kappa D_i\right)W}}-1\right]\times\frac{\sum_{i'\in\mathcal{I},i'\neq i} x_{i',k}p_{i',k}G_{i',k}\left|h_{i',k}\right|^2L_{i'}+\sum_{j\in\mathcal{J}} x_{j,k}p_{j,k}G_{j,k}\left|h_{j,k}\right|^2L_j+\sigma_0}{G_{i,k}\left|h_{i,k}\right|^2L_i} \tag{41}$$

$$\frac{\lambda_{i,k}D_ip_{i,k}}{W\log_2\left(1+\frac{p_{i,k}G_{i,k}|h_{i,k}|^2L_i}{\sum_{i'\in\mathcal{I},i'\neq i} x_{i',k}p_{i',k}G_{i',k}\left|h_{i',k}\right|^2L_{i'}+\sum_{j\in\mathcal{J}} x_{j,k}p_{j,k}^{\min}G_{j,k}\left|h_{j,k}\right|^2L_j+\sigma_0}\right)} \leq E_i-\kappa\left(f_i\right)^2D_i\left(1-\lambda_{i,k}\right) \tag{44}$$

where $\mathcal{W}(\cdot)$ is the Lambert-$\mathcal{W}$ function [47]. Ξ_A and Ξ_C are

$$\Xi_A = \left[E_i-\kappa\left(f_i\right)^2D_i\left(1-\lambda_i\right)\right]W \tag{46a}$$

$$\Xi_C = \lambda_{i,k}D_i\ln 2 \tag{46b}$$

and Ξ_F and Ξ_G can be given by (47) and (48). Thus, the optimal solution $p_{i,k}$ can be efficiently found by solving the problem $\mathbb{P}_6$.

D. RIS-assisted channel assignments

The RIS-assisted channel assignment subproblem aims at optimizing the channel assignment $\mathcal{X}$. For given beamwidth allocation Ω, offloading rate Λ and power allocation $\mathcal{P}$, the optimization problem $\mathbb{P}_2$ with respect to channel assignment can be reformulated as

$$\mathbb{P}_7: \{\mathcal{X}^*\} = \underset{\mathcal{X}}{\operatorname{argmin}}\left\{\tau_{\text{avg}} \mid \Omega^*, \Lambda^*, P^*\right\} \tag{49a}$$

$$s.t.\ \ x_{i,k}\in\{0,1\}, x_{j,k}\in\{0,1\}, \forall i\in\mathcal{I}, \forall j\in\mathcal{J}, \forall k\in\mathcal{K} \tag{49b}$$

$$\sum_{k\in\mathcal{K}} x_{i,k} = \sum_{k\in\mathcal{K}} x_{j,k} = 1, \forall i\in\mathcal{I}, \forall j\in\mathcal{J} \tag{49c}$$

$$\sum_{i\in\mathcal{I}} x_{i,k} + \sum_{j\in\mathcal{J}} x_{j,k} \leq M_k, \forall i\in\mathcal{I}, \forall j\in\mathcal{J} \tag{49d}$$

To solve the solution of problem $\mathbb{P}_7$, the channel matching algorithm is developed to reduce the co-channel interference. For the channel matching process, we define CP-ID set $\mathcal{I}$ and channel set $\mathcal{K}$, then the corresponding channel matching ϕ is given by

$$\forall i\in\mathcal{I},\ \phi(i)\in\mathcal{K},\ |\phi(i)|=1 \tag{50}$$

$$\forall k\in\mathcal{K},\ \phi(k)\in\mathcal{I},\ |\phi(t)|\leq M_k \tag{51}$$

Combining constraints (49b), (49c) and (49d), $\phi(i)=k$ implies that $x_{i,k}=1$, otherwise $x_{i,k}=0$. The utility functions for CP-ID i at k-th channel is

$$U_i = U_k = R_{i,\,k}, \tag{52}$$

where $R_{i,\,k}$ denote the transmission rate of CP-ID i at k-th channel. As the definition of utility functions, the relationships $\succ_i$ and $\succ_k$ should be satisfied the following requirements

$$i\succ_K i' \Leftrightarrow U_i(\phi) > U_{i'}\left(\phi'\right)$$
$$k\succ_i k' \Leftrightarrow U_k(\phi) > U_{k'}\left(\phi'\right).$$

Algorithm 1 RIS-assisted channel assignment algorithm

1: **Initialization**: Randomly initial IoT device, channel allocation $\mathcal{X}$ and swap matrix $\mathcal{C}$, where $\mathcal{C}=1-\mathcal{X}$
2: **for** $i\in\mathcal{M}$ **do**
3: **if** IoT device $i\in\mathcal{C}$ **do**
4: swapping the CP-ID with i, included in set $\mathcal{I}_{\text{swap}}$.
5: **if** there exists $i\in\mathcal{I}_{\text{swap}}$ **do**
6: i and i' leave the current channel and join other channel;
7: For allocation matrix $\mathcal{X}$, we have
8: $\mathcal{X}_{i,k}\leftarrow 0$, $\mathcal{X}_{i',k'}\leftarrow 1$
9: $\mathcal{X}_{i,k'}\leftarrow 1$, $\mathcal{X}_{i',k'}\leftarrow 0$
10: For allocation matrix $\mathcal{C}$, we have
11: $\mathcal{C}_{i,k}\leftarrow 0$, $\mathcal{C}_{i',k'}\leftarrow 0$
12: $\mathcal{C}_{i,k'}\leftarrow 0$, $\mathcal{C}_{i',k'}\leftarrow 0$
13: **end if**
14: **end if**
15: By given $\mathcal{X}$, update with Ω, P and Λ with Algorithm 2
16: **end for**

The detailed matching actions is provided in Alogrithm 1. Crossover and variation action: The CP-ID i assigned channel k execute crossover operation with CP-ID i' assigned channel k'.

Based on the above analysis, we provide the detailed implementation of the channel matching algorithm in Algorithm 1. The RIS-assisted channel assignment problem $\mathbb{P}_7$ is considered as the channel matching process, which means each CP-IDs is assigned to the corresponding fraction of the channel time. The optimal RIS-assisted channel assignment is obtained with two players-based matching iteration. Besides, the computational complexity of Algorithm 1 is given by assuming that in each iteration, the optimal matching selected from the preference list always conflicts with other matching results, then each CP-ID matches at most $\mathcal{K}$ subchannel, and its complexity is $\mathcal{O}(I\mathcal{K})$, where I is the number of CP-IDs. In addition, the complexity of updating the preference list for each CP-UE is $O(\mathcal{K}\log\mathcal{K})$. Hence, the complexity of Algorithm 1 can be expressed as $\mathcal{O}(I_{\text{iter}}(I\mathcal{K}+I\mathcal{K}\log\mathcal{K}))$, where I_{iter} is the number of iterations of point-to-point matching.

$$\Xi_F = -\frac{\lambda_{i,k} D_i \left(\sum_{i' \in \mathcal{I}, i' \neq i} x_{i',k} p_{i',k} G_{i',k} \left| h_{i',k} \right|^2 L_{i'} + \sum_{j \in \mathcal{J}} x_{j,\,k} p_{j,k}^{\min} G_{j,k} \left| h_{j,k} \right|^2 L_j + \sigma_0 \right)}{\left[E_i - \kappa \left(f_i \right)^2 D_i \left(1 - \lambda_{i,k} \right) \right] W G_{i,k} \left| h_{i,k} \right|^2 L_i} \tag{47}$$

$$\Xi_G = \frac{\sum_{i' \in \mathcal{I}, i' \neq i} x_{i',k} p_{i',k} G_{i',k} \left| h_{i',k} \right|^2 L_{i'} + \sum_{j \in \mathcal{J}} x_{j,k} p_{j,k}^{\min} G_{j,k} \left| h_{j,k} \right|^2 L_j + \sigma_0}{G_{i,k} \left| h_{i,k} \right|^2 L_i} \tag{48}$$

Algorithm 2 SCA-based alternating iterative algorithm

1: **Initialization**: Initial variables $\Omega^{(0)}$ and $\mathcal{P}^{(0)}$; set a termination threshold $\zeta > 0$ and $n = 0$

2: **while** $\tau_{\text{avg}}^{(n+1)} - \tau_{\text{avg}}^{(n)} > \zeta$ **do**

1) Solve problem $\mathbb{P}_3$ for given $\mathcal{X}$, P and Λ, and obtain the solution of beamwidth allocation $\mathbf{\Omega}$;
2) Solve problem $\mathbb{P}_5$ for given $\mathcal{X}$, $\mathcal{P}$ and $\mathbf{\Omega}$, and obtain the solution of offloading rate Λ;
3) Solve problem $\mathbb{P}_6$ for given $\mathcal{X}$, Λ and $\mathbf{\Omega}$, and obtain the solution of powers allocation $\mathcal{P}$;

4: **end while**

5: **Output** Ω, $\mathcal{P}$, Λ.

The Algorithm 2 consists four stages. In the first stage, Algorithm 1 is executed depending on the initialize variables Ω, $\mathcal{P}$ and Λ. Then, we update the beamwidth allocation Ω by given current matrix $\mathcal{X}$, $\mathcal{P}$ and Λ; In the third stage, we update the offloading rate Λ by given matrix $\mathcal{X}$, $\mathcal{P}$ and Ω; Finally, we update the power allocation $\mathcal{P}$ by given matrix $\mathcal{X}$, Λ and Ω.

IV. Simulation Results

In this section, we provide simulation results to verify the effectiveness of the RIS-assisted MEC-NOMA network. We consider one BSs to serve 20 IoT devices in the RIS-assisted network. The bandwidth of system is 100 MHz, which is available to the BSs. The direct and reflected channels are considered with independent and identically distributed Rayleigh fading. For the convenience of notation, Table I summarize the parameters used throughout the simulations. Based on 3GPPP standards, the channel path loss model is employed as $20 \log 10(\frac{4\pi}{\lambda}) + 10n \log 10(d) + \varphi$, where φ is the shadowing margin, n is the path loss exponent, λ is the carrier wavelength, and d is the distance from the transmitter to the receiver.

Firstly, we examine the performance of the proposed algorithm by taking three benchmark schemes: TDMA-MEC transmission scheme, NO RIS and GPM NOMA-MEC scheme [48]. We set the different main lobe gain of RIS as 3.6 and 25.6, respectively. An interesting observation from Fig. 2, when the number of input bits is relatively large, the proposed RIS-assisted MEC-NOMA offloading can achieve a significant energy consumption reduction, compared to other three schemes. The reason is that when the number of input data is large, the fraction of the channel assignment for the proposed offloading scheme can support the transmission of the IoT devices effectively. On the other hand, we can see that energy consumption decreases with the different main lobe gain of RIS. It is because RIS phases are optimized to improve the channel conditions between the BS and users. Furthermore, it can be seen that, as expected, the energy consumed by MEC-NOMA offloading increases as the number of input bits increases, which is due to the fact that a larger input bits lead to more transmitted data offloading, resulting in more energy to be consumed. It is also seen that the performance gap between the proposed MEC-NOMA

TABLE I
The proposed RIS-assisted MEC-NOMA framework parameters for simulation

Notation	Parameters	Value
W	System bandwidth	100 MHz
$g_{\text{RIS,n}}$	the main lobe gain of RIS	3.6, 25.6
T_p	Pilot transmission time	1 ms
$\mathcal{I}$	Sets of CP-IDs	{1,2...,I}
$\mathcal{J}$	Sets of CM-IDs	{1,2...,J}
z_{bs}	Side lobe gain of BS	0.001
z_{RIS}	Side lobe gain of RIS	0.001
σ_0^2/W	Noise power spectral density	-174 dBm/Hz

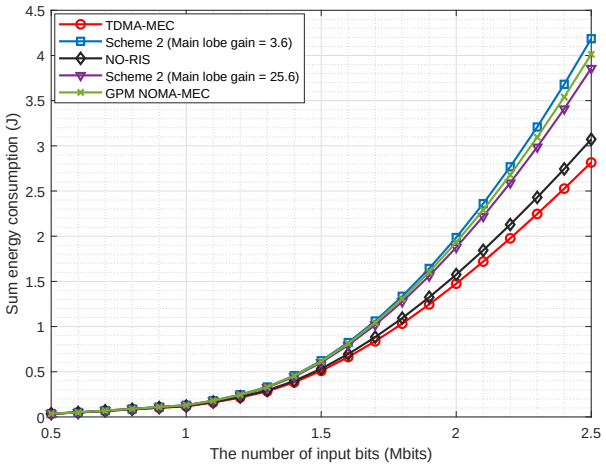

Fig. 2. The energy consumption versus the number of input bits for different schemes.

This article has been accepted for publication in IEEE Transactions on Communications. This is the author's version which has not been fully edited and content may change prior to final publication. Citation information: DOI 10.1109/TCOMM.2023.3277005

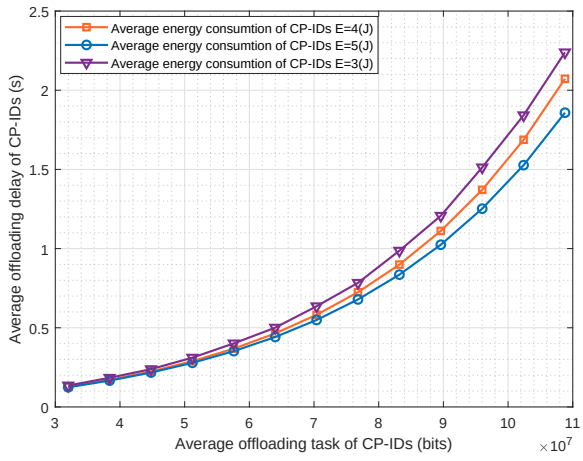

Fig. 3. The impact of offloading tasks on average offloading delay performance.

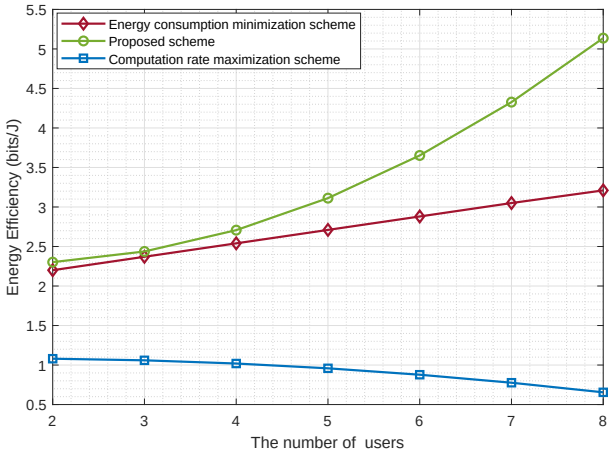

Fig. 5. Computation EE comparison versus the number of IoT devices.

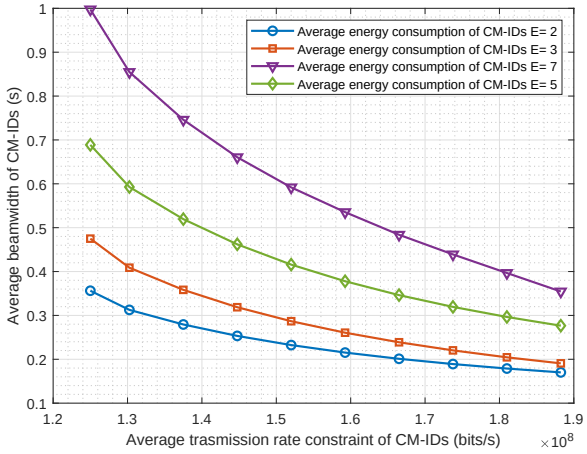

Fig. 4. Performance of CM-IDs under the proposed method.

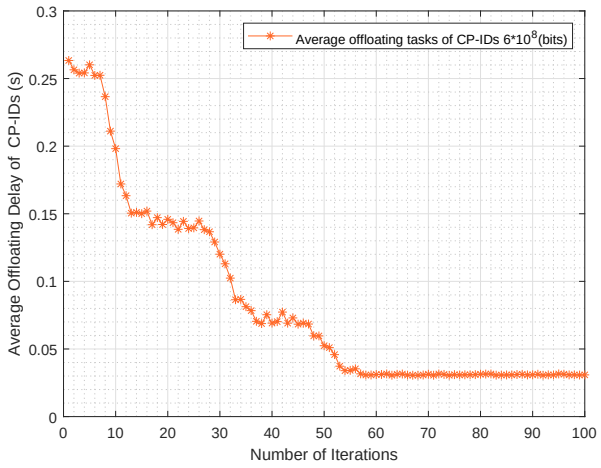

Fig. 6. The convergence performance of the proposed algorithm.

with multi-objective scheme and the conventional compared schemes increases as the number of channels increases, which is more beneficial to the application of RIS-assisted MEC-NOMA system. More importantly, it is shown that the performances of RIS-assisted MEC-NOMA offloading are always better than that of existing schemes, which elaborate the necessity of the channel assignment-based MEC-NOMA offloading in RIS-assisted communication scenarios.

In Fig. 3, different energy consumption E_{CP} is considered to evaluate the the average offloading tasks. It is observed that the obtained average offloading delay increases with offloading tasks of CP-IDs increases. It implies that the energy overhead of CP-IDs increases with the corresponding MEC-NOMA offloading tasks increasing, which resulting in CP-IDs cannot complete the tasks offloading within average delay of time. Therefore, practical channel assignment algorithm are crucial to RIS-assisted MEC-NOMA offloading.

To demonstrate the validity of task offloading, the relationship between the beamwidth allocation of the RIS-assisted MEC-NOMA scheme with different energy consumption E_{CP} is illustrated. As illustrated in Fig. 4, with average transmission rate increases, the beamwidth allocated to CM-IDs by the RIS-assisted MEC-NOMA will be reduced. The reason is that under certain transmission rate constraints, the problem $\mathbb{P}_0$ is transformed into the problem $\mathbb{P}_1$ in favour of reducing the delay of beam alignment. It can conclude that, the proposed RIS-assisted MEC-NOMA algorithm can fulfill the transmission requirements of CM-IDs under the tolerable range of offloading delay.

Fig. 5 plots the EE of the system versus the number of IoT devices under the proposed scheme, the energy consumption minimization scheme and the computation rate maximization scheme. It can be observed that the EE of system of the proposed scheme increases with the increasing IoT devices due to the fact that a larger $\mathcal{M}$ provides more flexibility for choosing IoT devices and allocating resources to achieve a higher EE of system, while the system computation EE under the computation rate maximization scheme shows a downward trend. From the curves, one can see that the proposed scheme outperforms other schemes, which verifies the superiority of the proposed scheme.

In Fig. 6, we provide the convergence of the RIS-assisted MEC-NOMA algorithm. After the RIS-assisted MEC-NOMA algorithm tended to stabilize about 52 iterations, which

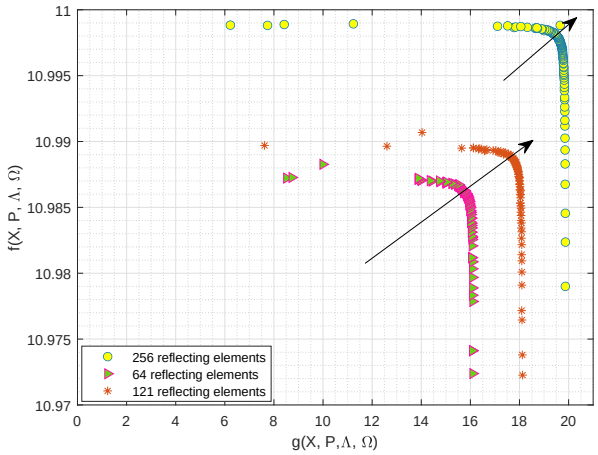

Fig. 7. System energy efficiency vs. spectral efficiency.

indicates the efficiency of proposed algorithms. As can be seen that the initial points is high. The reason is that at the initial iteration process, all of variables is generated randomly. Meanwhile, it is observed that for the curve of Fig. 6, there exist the sudden oscillation and irregularity in the first 52 iterations. This phenomenon is due to the channel matching mutation caused by the proposed algorithm, when the channel matching algorithm is executed.

Finally, an optimal point is provide to trade-off between maximizing $f(\mathcal{X},\mathcal{P},\Lambda,\Omega) = \frac{\sum_{i\in\mathcal{I}}\beta_i\tau_i}{I}$ and minimizing $g(\mathcal{X},\mathcal{P},\Lambda,\Omega) = \sum_{j\in\mathcal{J}}\sum_{k\in\mathcal{K}} x_{j,k}R_{j,k}$. Fig. 7 illustrates the trend of system $f(\mathcal{X},\mathcal{P},\Lambda,\Omega)$ with respect to $g(\mathcal{X},\mathcal{P},\Lambda,\Omega)$. It can be perceived that the tradeoff between $f(\mathcal{X},\mathcal{P},\Lambda,\Omega)$ and $g(\mathcal{X},\mathcal{P},\Lambda,\Omega)$ for different numbers of RIS reflecting elements, which confirms that $f(\mathcal{X},\mathcal{P},\Lambda,\Omega)$ and $g(\mathcal{X},\mathcal{P},\Lambda,\Omega)$ are conflicting objective functions. In fact, system throughput is by itself a function of system transmit power, thus any increase in the throughput may results in higher energy consumption as well. The point at optimal Pareto which energy consumption exceeds $g(\mathcal{X},\mathcal{P},\Lambda,\Omega)$ gains, the overall $f(\mathcal{X},\mathcal{P},\Lambda,\Omega)$ starts reducing. Furthermore, the tradeoff region is enlarged by increasing the number of RIS reflecting elements. This is the fact that for a ULA with ℓ antenna elements, the half power beamwidth can be expressed as $\theta(\ell) = 2\left(\frac{\pi}{2} - \arccos\frac{2.784}{\ell\pi}\right)$ [49]. According to (3), more reflecting elements can provide more antenna gain of signal transmission.

V. Conclusion

In this paper, we investigated the channel assignment-based task offloading for the RIS-assisted MEC-NOMA system, where the data transmission demands from both CM-IDs and CP-IDs were considered. For high task offloading demand, the channel resources are insufficient to assign one dedicated channel for each offloading IoT devices, which may cause strong interference in the transmitting procedure. The channel assignment-based MEC-NOMA task offloading approach is proposed for multiple applications offloading simultaneously through the fraction of the channel time scheme. Our objective is to minimizing the average delay of CP-IDs, while maximizing the transmission rate of CM-IDs. Based on that, the MOP for task offloading has been formulated, and joint four-stage iterative algorithm is developed to solve the formulated non-convex task offloading problem. Numerical results assess that performance improvement can be obtained by leveraging the channel assignment-based task offloading algorithm comparing with conventional schemes.

Appendix A
Proof of the Lemma 1

Proof: Firstly, the proof of the sufficiency is provided by defining

$$f_1(x) = \tau_{\text{avg}} ,$$
$$f_2(x) = -R_{\text{tot}} ,$$

where $x = (\mathcal{X},\mathcal{P},\Lambda,\Omega)$.

For a given ϵ, we assume that x^* is the unique optimal solution of the SOP, where x satisfies the constraints (21c) to $(21l)$. Thus, we have

$$f_1(x^*) \le f_1(x). \tag{53}$$

If x^* is not Pareto optimal solution of the MOP, the solution of problem SOP exist x' and $x' \neq x$ that satisfies

$$f_k(x') \le f_k(x^*), \quad \forall k = 1,2, \tag{54}$$

and there exist at least one $k \in \{1,2\}$ such that $f_k(x') < f_k(x^*)$. It is obviously that the contradicts with the uniqueness assumption. Hence, it concludes that x^* is Pareto optimal solution of the MOP.

Next, the proof of the necessity is provided. For $\epsilon = f_2(x^*)$, if x^* is a Pareto optimal solution for MOP and x^* is not the optimal solution for SOP, it exists a solution x', thus we have

$$f_1(x') \le f_1(x^*)$$

and

$$f_2(x') \le \epsilon = f_2(x^*).$$

This result also contradicts with the uniqueness assumption. The necessity is also proved. ■

References

[1] J. Tang, H. Tang, X. Zhang, K. Cumanan, G. Chen, K.-K. Wong, and J. A. Chambers, "Energy minimization in D2D-assisted cache-enabled internet of things: A deep reinforcement learning approach," *IEEE Transactions on Industrial Informatics*, vol. 16, no. 8, pp. 5412–5423, 2020.

[2] A. u. R. Khan, M. Othman, S. A. Madani, and S. U. Khan, "A survey of mobile cloud computing application models," *IEEE Communications Surveys and Tutorials*, vol. 16, no. 1, pp. 393–413, 2014.

[3] X. Chen, L. Jiao, W. Li, and X. Fu, "Efficient multi-user computation offloading for mobile-edge cloud computing," *IEEE/ACM Transactions on Networking*, vol. 24, no. 5, pp. 2795–2808, 2016.

[4] X. Cao, F. Wang, J. Xu, R. Zhang, and S. Cui, "Joint computation and communication cooperation for energy-efficient mobile edge computing," *IEEE Internet of Things Journal*, vol. 6, no. 3, pp. 4188–4200, 2019.

[5] B. Liu, C. Liu, and M. Peng, "Resource allocation for energy-efficient MEC in NOMA-enabled massive IoT networks," *IEEE Journal on Selected Areas in Communications*, vol. 39, no. 4, pp. 1015–1027, 2021.

[6] S. Mao, S. Leng, S. Maharjan, and Y. Zhang, "Energy efficiency and delay tradeoff for wireless powered mobile-edge computing systems with multi-access schemes," *IEEE Transactions on Wireless Communications*, vol. 19, no. 3, pp. 1855–1867, 2020.

[7] X. Hu, K.-K. Wong, and K. Yang, "Wireless powered cooperation-assisted mobile edge computing," *IEEE Transactions on Wireless Communications*, vol. 17, no. 4, pp. 2375–2388, 2018.

[8] H. Ding, Y. Guo, X. Li, and Y. Fang, "Beef up the edge: Spectrum-aware placement of edge computing services for the internet of things," *IEEE Transactions on Mobile Computing*, vol. 18, no. 12, pp. 2783–2795, 2019.

[9] X. He, R. Jin, and H. Dai, "Physical-layer assisted secure offloading in mobile-edge computing," *IEEE Transactions on Wireless Communications*, vol. 19, no. 6, pp. 4054–4066, 2020.

[10] Z. Chen, J. Tang, X. Y. Zhang, D. K. C. So, S. Jin, and K.-K. Wong, "Hybrid evolutionary-based sparse channel estimation for IRS-assisted mmwave MIMO systems," *IEEE Transactions on Wireless Communications*, vol. 21, no. 3, pp. 1586–1601, 2022.

[11] C. Huang, A. Zappone, G. C. Alexandropoulos, M. Debbah, and C. Yuen, "Reconfigurable intelligent surfaces for energy efficiency in wireless communication," *IEEE Transactions on Wireless Communications*, vol. 18, no. 8, pp. 4157–4170, 2019.

[12] M. He, W. Xu, H. Shen, G. Xie, C. Zhao, and M. Di Renzo, "Cooperative multi-RIS communications for wideband mmwave MISO-OFDM systems," *IEEE Wireless Communications Letters*, vol. 10, no. 11, pp. 2360–2364, 2021.

[13] Y. Yang, Y. Gong, and Y.-C. Wu, "Intelligent-reflecting-surface-aided mobile edge computing with binary offloading: Energy minimization for IoT devices," *IEEE Internet of Things Journal*, vol. 9, no. 15, pp. 12973–12983, 2022.

[14] L. Zhang, Y. Wang, W. Tao, Z. Jia, T. Song, and C. Pan, "Intelligent reflecting surface aided MIMO cognitive radio systems," *IEEE Transactions on Vehicular Technology*, vol. 69, no. 10, pp. 11445–11457, 2020.

[15] Z. Li, M. Chen, Z. Yang, J. Zhao, Y. Wang, J. Shi, and C. Huang, "Energy efficient reconfigurable intelligent surface enabled mobile edge computing networks with noma," *IEEE Transactions on Cognitive Communications and Networking*, vol. 7, no. 2, pp. 427–440, 2021.

[16] T. Bai, C. Pan, C. Han, and L. Hanzo, "Reconfigurable intelligent surface aided mobile edge computing," *IEEE Wireless Communications*, vol. 28, no. 6, pp. 80–86, 2021.

[17] J. Gozalvez, "New 3GPP standard for IoT [mobile radio]," *IEEE Vehicular Technology Magazine*, vol. 11, no. 1, pp. 14–20, 2016.

[18] M. Vaezi, R. Schober, Z. Ding, and H. V. Poor, "Non-orthogonal multiple access: Common myths and critical questions," *IEEE Wireless Communications*, vol. 26, no. 5, pp. 174–180, 2019.

[19] A. E. Mostafa, Y. Zhou, and V. W. Wong, "Connection density maximization of narrowband iot systems with NOMA," *IEEE Transactions on Wireless Communications*, vol. 18, no. 10, pp. 4708–4722, 2019.

[20] W. Xu, Y. Cui, H. Zhang, G. Y. Li, and X. You, "Robust beamforming with partial channel state information for energy efficient networks," *IEEE Journal on Selected Areas in Communications*, vol. 33, no. 12, pp. 2920–2935, 2015.

[21] W. Xu, J. Liu, S. Jin, and X. Dong, "Spectral and energy efficiency of multi-pair massive MIMO relay network with hybrid processing," *IEEE Transactions on Communications*, vol. 65, no. 9, pp. 3794–3809, 2017.

[22] L. P. Qian, A. Feng, Y. Huang, Y. Wu, B. Ji, and Z. Shi, "Optimal SIC ordering and computation resource allocation in MEC-aware NOMA NB-IoT networks," *IEEE Internet of Things Journal*, vol. 6, no. 2, pp. 2806–2816, 2019.

[23] G. Cui, Q. He, X. Xia, F. Chen, F. Dong, H. Jin, and Y. Yang, "OL-EUA: Online user allocation for NOMA-based mobile edge computing," *IEEE Transactions on Mobile Computing*, pp. 1–1, 2021.

[24] A. Kiani and N. Ansari, "Edge computing aware NOMA for 5G networks," *IEEE Internet of Things Journal*, vol. 5, no. 2, pp. 1299–1306, 2018.

[25] X. Pei, H. Yu, X. Wang, Y. Chen, M. Wen, and Y.-C. Wu, "NOMA-based pervasive edge computing: Secure power allocation for IoV," *IEEE Transactions on Industrial Informatics*, vol. 17, no. 7, pp. 5021–5030, 2021.

[26] B. Li, F. Si, W. Zhao, and H. Zhang, "Wireless powered mobile edge computing with NOMA and user cooperation," *IEEE Transactions on Vehicular Technology*, vol. 70, no. 2, pp. 1957–1961, 2021.

[27] H. Yin, X. Zhang, H. H. Liu, Y. Luo, C. Tian, S. Zhao, and F. Li, "Edge provisioning with flexible server placement," *IEEE Transactions on Parallel and Distributed Systems*, vol. 28, no. 4, pp. 1031–1045, 2017.

[28] Y. Wu, K. Ni, C. Zhang, L. P. Qian, and D. H. K. Tsang, "NOMA-assisted multi-access mobile edge computing: A joint optimization of computation offloading and time allocation," *IEEE Transactions on Vehicular Technology*, vol. 67, no. 12, pp. 12244–12258, 2018.

[29] M. Hua, H. Tian, X. Lyu, W. Ni, and G. Nie, "Online offloading scheduling for noma-aided mec under partial device knowledge," *IEEE Internet of Things Journal*, vol. 9, no. 3, pp. 2227–2241, 2022.

[30] J. Feng, Q. Pei, F. R. Yu, X. Chu, J. Du, and L. Zhu, "Dynamic network slicing and resource allocation in mobile edge computing systems," *IEEE Transactions on Vehicular Technology*, vol. 69, no. 7, pp. 7863–7878, 2020.

[31] Y. Wu, L. Qian, J. Ouyang, W. Lu, B. Lin, and Z. Shi, "Non-orthogonal multiple access assisted mobile edge computing via device-to-device communications," in *2020 IEEE 92nd Vehicular Technology Conference (VTC2020-Fall)*, pp. 1–6, 2020.

[32] T. Bai, C. Pan, Y. Deng, M. Elkashlan, A. Nallanathan, and L. Hanzo, "Latency minimization for intelligent reflecting surface aided mobile edge computing," *IEEE Journal on Selected Areas in Communications*, vol. 38, no. 11, pp. 2666–2682, 2020.

[33] S. Huang, S. Wang, R. Wang, M. Wen, and K. Huang, "Reconfigurable intelligent surface assisted mobile edge computing with heterogeneous learning tasks," *IEEE Transactions on Cognitive Communications and Networking*, vol. 7, no. 2, pp. 369–382, 2021.

[34] T. Bai, C. Pan, H. Ren, Y. Deng, M. Elkashlan, and A. Nallanathan, "Resource allocation for intelligent reflecting surface aided wireless powered mobile edge computing in ofdm systems," *IEEE Transactions on Wireless Communications*, vol. 20, no. 8, pp. 5389–5407, 2021.

[35] X. Hu, C. Masouros, and K.-K. Wong, "Reconfigurable intelligent surface aided mobile edge computing: From optimization-based to location-only learning-based solutions," *IEEE Transactions on Communications*, vol. 69, no. 6, pp. 3709–3725, 2021.

[36] S. Mao, J. Wu, L. Liu, D. Lan, and A. Taherkordi, "Energy-efficient cooperative communication and computation for wireless powered mobile-edge computing," *IEEE Systems Journal*, vol. 16, no. 1, pp. 287–298, 2022.

[37] A. Goldsmith, *Wireless Communications*. Cambridge, U.K.: Cambridge Univ. Press,, 2007.

[38] Q. Wu and R. Zhang, "Intelligent reflecting surface enhanced wireless network via joint active and passive beamforming," *IEEE Transactions on Wireless Communications*, vol. 18, no. 11, pp. 5394–5409, 2019.

[39] S. Zhou, L. Chen, and W. Wang, "Attitude information aided mmwave beam tracking based on codebook," *IEEE Communications Letters*, vol. 26, no. 5, pp. 1160–1164, 2022.

[40] Y. Zhang, H.-M. Wang, T.-X. Zheng, and Q. Yang, "Energy-efficient transmission design in non-orthogonal multiple access," *IEEE Transactions on Vehicular Technology*, vol. 66, no. 3, pp. 2852–2857, 2017.

[41] J. Wildman, P. H. J. Nardelli, M. Latva-aho, and S. Weber, "On the joint impact of beamwidth and orientation error on throughput in directional wireless poisson networks," *IEEE Transactions on Wireless Communications*, vol. 13, no. 12, pp. 7072–7085, 2014.

[42] J. Shi, W. Yu, Q. Ni, W. Liang, Z. Li, and P. Xiao, "Energy efficient resource allocation in hybrid non-orthogonal multiple access systems," *IEEE Transactions on Communications*, vol. 67, no. 5, pp. 3496–3511, 2019.

[43] E. C. Cejudo, H. Zhu, and J. Wang, "Resource allocation in multicarrier NOMA systems based on optimal channel gain ratios," *IEEE Transactions on Wireless Communications*, vol. 21, no. 1, pp. 635–650, 2022.

[44] D. Wang, N. Zhang, Z. Li, F. Gao, and X. Shen, "Leveraging high order cumulants for spectrum sensing and power recognition in cognitive radio networks," *IEEE Transactions on Wireless Communications*, vol. 17, no. 2, pp. 1298–1310, 2018.

[45] Z. Zhao, J. Shi, Z. Li, J. Si, P. Xiao, and R. Tafazolli, "Multi-objective resource allocation for mmwave MEC offloading under competition of communication and computing tasks," *IEEE Internet of Things Journal*, pp. 1–1, 2021.

[46] Y. Wang, M. Sheng, X. Wang, L. Wang, and J. Li, "Mobile-edge computing: Partial computation offloading using dynamic voltage scaling," *IEEE Transactions on Communications*, vol. 64, no. 10, pp. 4268–4282, 2016.

[47] M. Zeng, W. Hao, O. A. Dobre, and H. V. Poor, "Delay minimization for massive MIMO assisted mobile edge computing," *IEEE Transactions on Vehicular Technology*, vol. 69, no. 6, pp. 6788–6792, 2020.

[48] L. He, M. Wen, Y. Chen, M. Yan, and B. Jiao, "Delay aware secure offloading for NOMA-assisted mobile edge computing in internet of vehicles," *IEEE Transactions on Communications*, vol. 70, no. 8, p-p. 5271–5284, 2022.

[49] Y. Quan, J.-M. Klif, and M. Coupechoux, "Spatio-temporal wireless D2D network with beamforming," in *ICC 2021 - IEEE International Conference on Communications*, pp. 1–6, 2021.